Chemistry–A European Journal
Research Article
doi.org/10.1002/chem.202202943
Chemistry Europe
European Chemical Societies Publishing
www.chemeurj.org

IR/UV Double Resonance Study of the 2-Phenylallyl Radical and its Pyrolysis Products

Tobias Preitschopf,[a] Floriane Sturm,[a] Iuliia Stroganova,[c] Alexander K. Lemmens,[b] Anouk M. Rijs,*[c] and Ingo Fischer*[a]

Abstract: Isolated 2-phenylallyl radicals (2-PA), generated by pyrolysis from a nitrite precursor, have been investigated by IR/UV ion dip spectroscopy using free electron laser radiation. 2-PA is a resonance-stabilized radical that is considered to be involved in the formation of polycyclic aromatic hydrocarbons (PAH) in combustion, but also in interstellar space. The radical is identified based on its gas-phase IR spectrum. Furthermore, a number of bimolecular reaction products are identified, showing that the self-reaction as well as reactions with unimolecular decomposition products of 2-PA form several PAH efficiently. Possible mechanisms are discussed and the chemistry of 2-PA is compared with the one of the related 2-methylallyl and phenylpropargyl radicals.

Introduction

To understand the formation of polycyclic aromatic hydrocarbons (PAH) and soot is still a challenging task for chemistry. In high temperature processes, in particular combustion, one tries to avoid formation of these carcinogenic and environmentally harmful molecules as much as possible.[1] On the other hand, in astrochemistry PAH are considered as likely carriers of the unidentified infrared bands (UIR), emission bands characteristic for aromatic molecules and PAH.[2] The most important pathways to PAH formation have been reviewed recently,[3] among them the HACA (hydrogen abstraction C_2H_2 addition) and the PAC (phenyl addition (dehydro-)cyclization) mechanisms. However, almost all models agree on the central role of resonantly stabilized radicals (RSR) in the growth of aromatic species.[4] RSR can accumulate in reactive environments due to their lower reactivity towards O_2 and therefore be involved in secondary reactions.[5] Hence, the spectroscopic identification of RSR and the investigation of their chemistry is of considerable interest. Here, we focus on reactions of the 2-phenylallyl radical, **2** in Scheme 1, and compare its high temperature chemistry with the one of the related 2-methylallyl[6] and phenylpropargyl radicals.[7] While for its isomer 1-phenylallyl, a study of the $D_1 \leftarrow D_0$ transition by laser-induced fluorescence has been reported,[8] no spectroscopic information is available so far on **2**. Theoretical work is limited to studies on reactions of chemically activated C_9H_9 isomers.[9] This lack of information hampers *in situ* detection in reactive environments. Thus, laboratory experiments on isolated radicals under well-defined conditions are required to get more insight into the chemistry of RSR. Thermal reactions in pyrolysis microreactors are well suited to generate reactive molecules cleanly and at a sufficiently high number density to conduct gas-phase experiments.[10] The properties of such a microreactor were recently modeled using fluid dynamics simulations.[11] Depending on the mode of operation and the choice of parameters (backing gas pressure, length of the heated region and time delay between laser and gas pulse), such microreactors can be used to characterize isolated radicals, but also serve to initiate unimolecular and bimolecular chemical reactions.[11–12] In the present work we employed this technique to generate **2** from 3-phenylbut-3-en-1-yl nitrite (**1**), as visible in Scheme 1. Reaction products are often characterized by photoionization with tunable synchrotron radiation, either using the ionization energy (IE) derived from ion yields for identification[13]

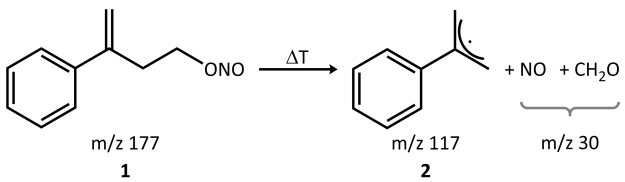

Scheme 1. Pyrolysis of 3-phenylbut-3-en-1-yl nitrite **1** is used to generate the 2-phenylallyl radical **2**.

[a] *T. Preitschopf, F. Sturm, Prof. Dr. I. Fischer*
Institute of Physical and Theoretical Chemistry
University of Würzburg
Am Hubland, 97074 Würzburg (Germany)
E-mail: ingo.fischer@uni-wuerzburg.de

[b] *Dr. A. K. Lemmens*
Institute for Molecules and Materials, FELIX Laboratory
Radboud University
Toernooiveld 7, 6525 ED Nijmegen (The Netherlands)

[c] *I. Stroganova, Prof. Dr. A. M. Rijs*
Division of BioAnalytical Chemistry
AIMMS Amsterdam Institute of Molecular and Life Sciences
Faculty of Science
Vrije Universiteit Amsterdam
De Boelelaan 1081, 1081 HV Amsterdam (The Netherlands)
E-mail: a.m.rijs@vu.nl

Supporting information for this article is available on the WWW under https://doi.org/10.1002/chem.202202943

or photoelectron spectra.[14] IR/UV ion dip spectroscopy is an alternative tool to characterize reaction products, because it combines the structural sensitivity of infrared spectroscopy with mass information.[15] It is particularly well suited for the isomer-selective characterization of aromatic molecules and PAH, which generally absorb in the UV. Recently, we employed IR/UV spectroscopy to record IR spectra of isolated RSR with relevance to combustion and to monitor their chemical reactions, among them phenylpropargyl,[7] benzyl,[16] *ortho*-benzyne[17] and 2-methylallyl.[6] In contrast, small molecules without a UV chromophore are difficult to detect by IR/UV, thus complementary photoionization data are helpful, as shown for the *ortho*-benzyne self-reaction.[17] As an alternative to pyrolysis, electrical discharges have been employed to generate RSR and follow their chemistry. Recently, a discharge of naphthalene has been utilized to study the formation of PAH by IR/UV spectroscopy.[18]

Results

Mass spectra

SPI TOF-MS: The single-photon ionization (SPI) time-of-flight mass spectrum of the pyrolysis products, recorded using synchrotron radiation at the Swiss Light Source (SLS), is presented in Figure 1a. The spectrum gives an approximate distribution of the relative molecular concentrations in the jet.[19] At around 800 K, an almost complete conversion of **1** (m/z 177) and a relative intense signal at m/z 117, corresponding to the mass of **2**, are observed. In addition, a small signal is visible at m/z 30 due to NO, confirming the decomposition shown in Scheme 1. Contributions of formaldehyde (CH_2O) can be excluded due to its high IE.[20] Addition of an H atom to **2** leads to the most dominant peak at m/z 118, while H atom loss results in m/z 116. Dimerization of **2** is evident from the signal at m/z 234. Several further signals such as m/z 78, 92, or 104, indicate that small aromatics are formed in the unimolecular

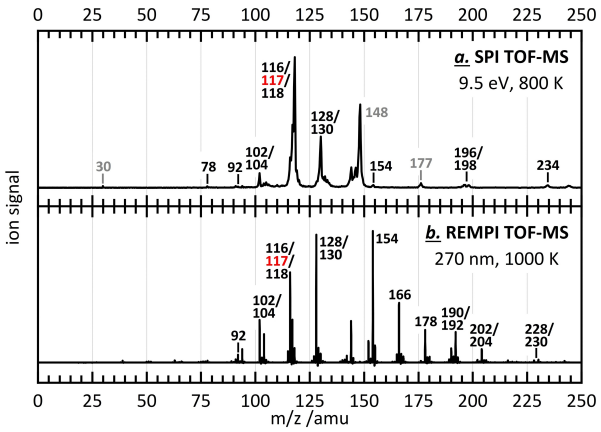

Figure 1. Time-of-flight mass spectra (TOF-MS) of **1** with pyrolysis recorded at 9.5 eV in a single-photon ionization process (SPI) at T_{pyro} around 800 K (trace a) and at 270 nm (4.59 eV) in a [1 + 1]-REMPI process at T_{pyro} around 1000 K (b).

decomposition of **2** and might contribute to the formation of higher (polycyclic) aromatic hydrocarbons as suggested by m/z 128 or 154. Further mass spectra with and without pyrolysis are given in Figure S1 in the Supporting Information.

REMPI TOF-MS: Figure 1b depicts the [1 + 1]-REMPI mass spectrum at around 1000 K. The higher pyrolysis temperature was chosen to promote bimolecular reactions in the microreactor.[11–12] At the excitation wavelength of 270 nm (4.59 eV), many PAH possess absorption bands,[21] that lead to enhanced signal intensities in comparison with the SPI spectrum (see for instance m/z 92, 104, 116, 128, or 154). Commonly, the strong $S_3 \leftarrow S_0$ and/or the medium strong $S_2 \leftarrow S_0$ transitions of the vast majority of PAH lie around this wavelength region.[21b] Hence, excitation around 270 nm is ideal to monitor a large number of aromatic high-temperature reaction products. In addition, sufficient absorption of **2** at this wavelength is secured (see Figure S2). In comparison with the SPI TOF-MS (trace a), higher masses are visible due to the high sensitivity of resonant photoionization.[21b] Note, that the mass-to-charge ratio of many of the peaks differs by 76 amu in comparison with signals at lower m/z (e.g., m/z 102 and 178, 116 and 192, 128 and 204, 154 and 230). This indicates that molecular growth is dominated by addition of phenyl radicals (accompanied with a loss of an H atom), which is followed by dehydrocyclization (H_2 loss) as suggested by the signals at m/z 190 and 192, 202 and 204, 228 and 230.

The corresponding REMPI excitation spectra (260–280 nm) recorded at a pyrolysis temperature of 1000 K exhibit unstructured and broadened UV features due to overlapping bands of the pyrolysis products,[15] which impedes isomer identification. Note that the molecules are cooled in the jet expansion, but possibly to room temperature only.

IR/UV spectra

In the following section, we present mass-selected IR/UV spectra in combination with quantum chemical calculations of vibrational spectra, that allow to unambiguously identify the mass signals observed in the REMPI TOF-MS (cf. Figure 1b). Several additional spectra are presented in the Supporting Information. The width of the vibrational absorption bands is mostly determined by power broadening owing to the intense IR radiation and the rotational temperature of the pyrolysis products. Most reaction products are present in the temporal center of the gas pulse, where rotational cooling is less effective. Note, that narrow electronic transitions are not crucial to obtain an ion depletion signal, since IR excitation can result in large variations of the UV absorption cross section even for broad bands.[22] Additionally, the high IR intensity facilitates absorption of further IR photons, possibly leading to fragmentation.[23] As absorption of the first IR photon remains the bottleneck for the process, ground state IR spectra are obtained.

m/z 117 and 118: Figure 2a presents the IR/UV spectrum of m/z 117 obtained from pyrolysis of **1** (see Scheme 1) at around 800 K. A depletion of 15–20% was observed for the most

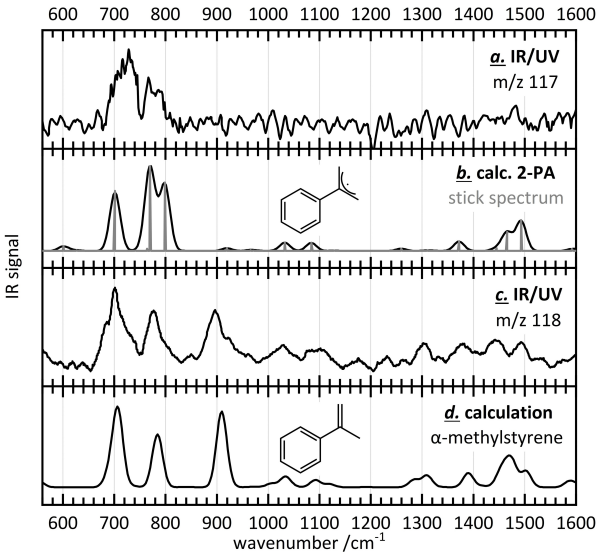

Figure 2. The IR/UV spectrum of m/z 117 (trace a) is assigned to **2** based on comparison with a computed spectrum (b). Addition of an H atom leads to the formation of α-methylstyrene as shown in traces c and d.

dominant band at 721 cm^{-1}. The wavenumber of the peak centre was determined using Gaussian fitting. The band is well represented in the computed IR spectrum of **2** (trace 2b) and is assigned to the aryl C–H out-of-plane wagging vibration. Two further distinct bands are identified at 767 and 786 cm^{-1}, originating from an out-of-plane wagging mode and the symmetric CH_2 out-of-plane bending vibration. Note, that the latter is in excellent agreement with the wavenumber of the CH_2 out-of-plane bending mode of the related 2-methylallyl radical.[6] Several further bands of smaller and medium intensity are predicted in the higher wavenumber region by the computation, but are difficult to identify in the experimental spectrum due to the low S/N ratio. To exclude (partial) isomerization of **2** in the microreactor, the experimental data are compared to computed IR spectra of the *E*- and *Z*-1-phenylallyl radical (see Figure S3 in the Supporting Information). A disagreement is evident.

A threshold photoelectron spectrum (TPES) of **2**, recorded at the SLS, is given in Figure S4. The spectrum is broad and unstructured due to the large geometry change upon ionization (see Figure S5). It is therefore only discussed in the Supporting Information. Here, we just note that an adiabatic IE of 7.6 ± 0.1 eV has been determined.

The mass signal at m/z 118 (Figure 1b) already indicates addition of an H atom to **2**. The corresponding experimental and computed IR spectra (see Figure 2c and d) confirm the formation of α-methylstyrene (C_9H_{10}). The absence of the band at around 900 cm^{-1} in trace 2a rules out that the signal of m/z 117 originates from dissociative photoionization of m/z 118, with its otherwise rather similar IR spectrum.

m/z 228 and 230: The peak at m/z 230 is one of the most interesting signals in the REMPI TOF-MS (Figure 1b) as it corresponds to direct dimerization of **2** to m/z 234 (see Figure 1a) followed by dehydrocyclization, a pattern previously observed for 2-methylallyl radicals.[6] Based on comparison with computed IR spectra of terphenyl isomers (Figure 3d–f), the corresponding IR/UV spectrum (Figure 3c) is best represented by *p*-terphenyl ($C_{18}H_{14}$) in terms of the energetic positions and relative intensities of the vibrational bands. In particular, the characteristic band at 842 cm^{-1}, the C–H out-of-plane wagging vibration of the central aromatic ring, is only present in the computed spectrum of *p*-terphenyl. The formation of *m*-terphenyl is excluded by the computed band at 621 cm^{-1}, which is absent in the experimental spectrum, while contributions of *o*-terphenyl are small at best. Note, that the latter is slightly higher in energy than *p*- and *m*-terphenyl which are almost degenerate and constitute the lowest energy structures at 1000 K. Interestingly, the *para* isomer was also observed as a dimerization product of phenylpropargyl radicals.[7]

The IR/UV spectrum of m/z 228 (Figure 3a) is readily assigned to triphenylene ($C_{18}H_{12}$, trace 3b) by the small number of vibrational transitions due to the high symmetry (D_{3h}) and its distinctive C–H out-of-plane wagging vibration (in-phase) at 731 cm^{-1}. The observation of triphenylene suggests the formation of *o*-terphenyl as an intermediate, followed by dehydrocyclization (-H_2) into the more stable condensed PAH.[3,24]

m/z 154 and 178: Phenyl chemistry in the microreactor is further indicated by the spectrum of m/z 154 (Figure 4a). In addition to the characteristic C–H out-of-plane bending vibrations at 699, 736, and 767 cm^{-1}, the spectrum exhibits several further features, for example, at 612 or 1480 cm^{-1}, that

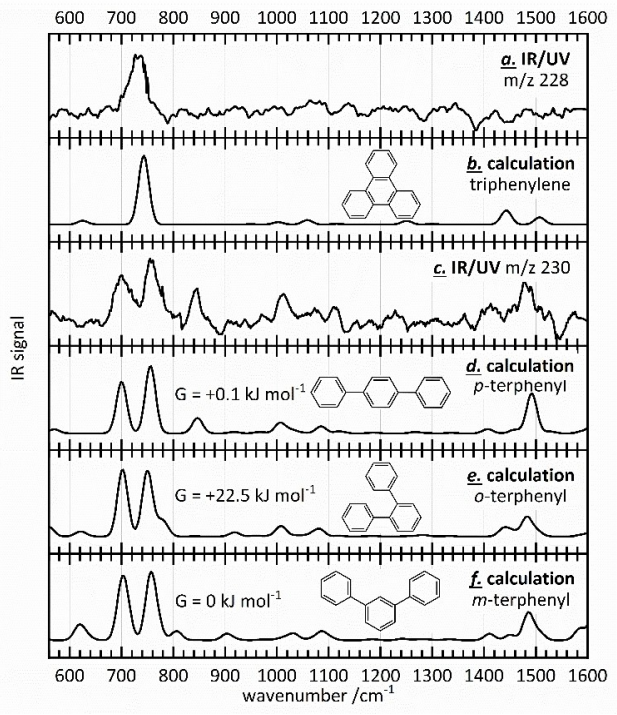

Figure 3. The IR/UV spectrum of m/z 228 (trace a) is due to triphenylene (b), whereas the one of m/z 230 (c) is dominated by p-terphenyl (d). Contributions of the thermochemically less stable ortho isomer (e) are small at best and conclusively presumed by the generation of triphenylene

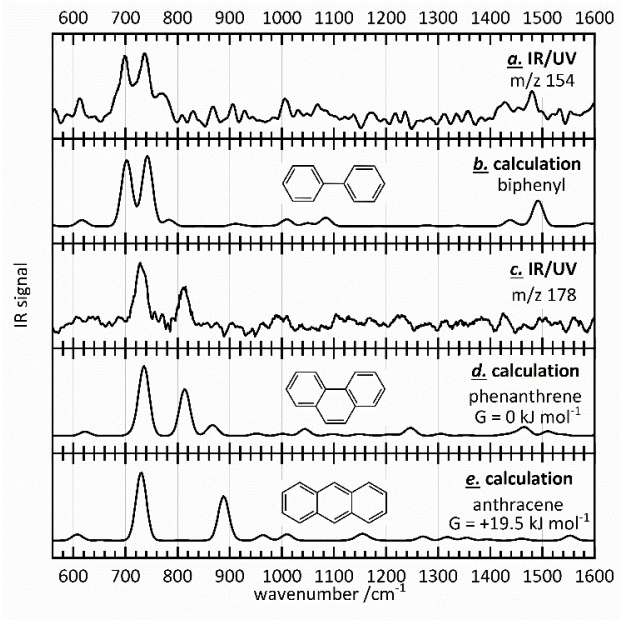

Figure 4. The carrier of the IR/UV spectrum of m/z 154 is identified as biphenyl (traces a and b). M/z 178 (c) is assigned to the thermochemically more stable phenanthrene (d).

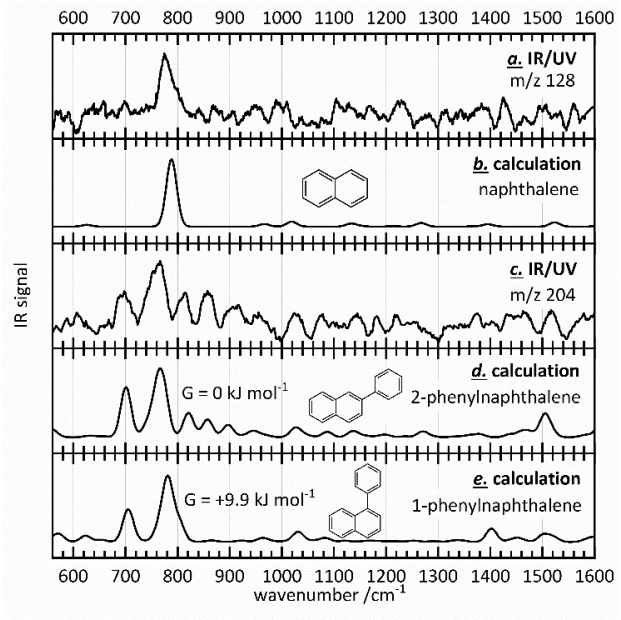

Figure 5. The structural information of the IR/UV spectrum of m/z 128 facilitates unambiguous assignment of naphthalene (traces a and b). The IR/UV spectrum of m/z 204 (c) is best represented by the thermochemically more stable 2-phenylnaphthalene (d).

permit an unambiguous assignment to biphenyl ($C_{12}H_{10}$, trace 4b).

The mass-selected IR/UV spectrum of m/z 178 (Figure 4c) displays the formation of phenanthrene ($C_{14}H_{10}$), as the two dominant bands at 730 and 812 cm^{-1} are in excellent agreement with the computed spectrum (trace 4d). Contributions of the thermochemically less stable isomer anthracene are ruled out by the absence of its prominent C–H out-of-plane wagging vibration at 889 cm^{-1} in the spectrum (trace 4e).

m/z 128 and 204: Based on comparison with a computed IR spectrum, the IR/UV spectrum of m/z 128 (Figure 5a) is dominated by the characteristic C–H out-of-plane wagging vibration (in-phase) at 779 cm^{-1} of naphthalene ($C_{10}H_8$, trace 5b). No further vibrational bands are observed in the spectrum, so the PAH is readily assigned as the only carrier of m/z 128.

The mass signal at m/z 204 in the REMPI TOF-MS (cf. Figure 1b) is closely related to m/z 128 as both peaks are separated by 76 amu. This suggests the addition of a phenyl radical to naphthalene, resulting in the formation of the two possible isomers 1- and 2-phenylnaphthalene ($C_{16}H_{12}$). A comparison of the corresponding IR/UV spectrum (Figure 5c) with the computed IR spectrum (trace 5d) verifies the generation of 2-phenylnaphthalene in the reactor, as spacing and relative intensities of the most intense out-of-plane wagging vibrations between 670 to 940 cm^{-1} agree well. Formation of the thermochemically less stable 1-phenylnaphthalene is unlikely, because the most dominant band at 782 cm^{-1} is predicted at higher wavenumbers (trace 5e) compared with the predominant band of 2-phenylnaphthalene (shift ~15 cm^{-1}).

Additional observed masses: Several further mass signals were assigned based on the IR/UV spectra shown in the Supporting Information. Among them are m/z 102 and 104 identified as phenylacetylene and styrene (see Figure S6), m/z 116 assigned to indene (Figure S7), and m/z 166 identified as fluorene (Figure S8).

Discussion

Three key reactions of **2** are involved in molecular growth as summarized in Scheme 2. At around 800 K, the radical self-reaction, **A** in Scheme 2, sets in as apparent from the mass peak at m/z 234 in the SPI TOF-MS (Figure 1a). A heat of reaction $\Delta_R H^\circ = -193$ kJ mol^{-1} was computed for the exothermic reaction. The reaction product 2,5-diphenyl-1,5-hexadiene (**3**) with a computed IE of 7.46 eV was not identified by IR/UV ion dip spectroscopy, possibly due to a low UV absorption cross section at the excitation wavelength. However, its formation is concluded from the formation of *p*-terphenyl (m/z 230), see Figure 3c. The latter is most likely formed in a Cope rearrangement of **3** via a cyclic, diradical intermediate followed by aromatization as suggested in theoretical studies.[25] A $\Delta_R H^\circ = -45$ kJ mol^{-1} was computed for the reaction that is accompanied by the entropically favorable loss of two hydrogen molecules.

At around 1000 K, dimerization competes with unimolecular decomposition of **2** to a phenyl radical and likely allene, see reaction **B** in Scheme 2 ($\Delta_R H^\circ = +222$ kJ mol^{-1}). The presence of significant amounts of phenyl in the microreactor is evident as several reaction products identified by IR/UV ion dip spectro-

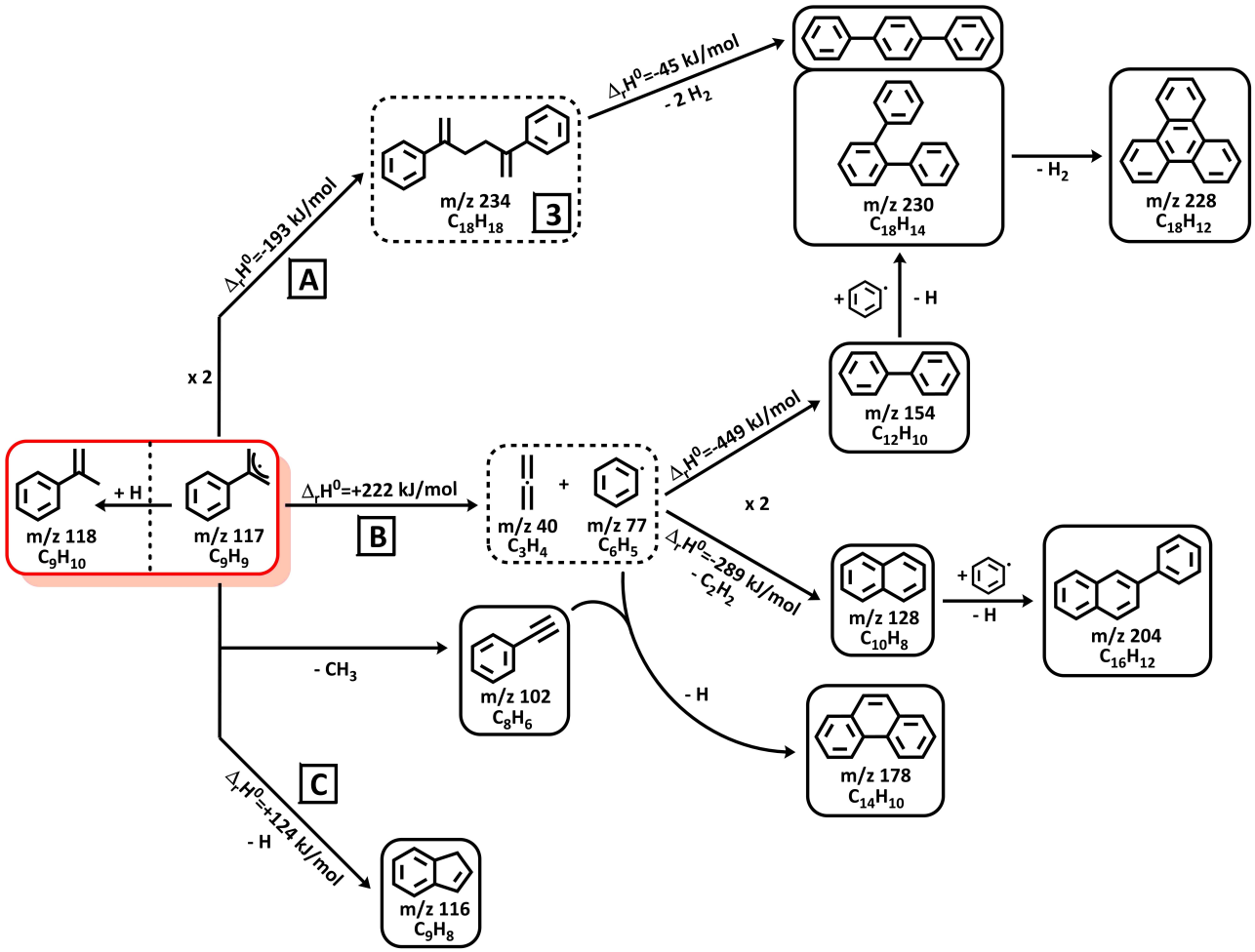

Scheme 2. High temperature reaction products of **2** in a flow microreactor identified by IR/UV ion dip spectroscopy (in black). Molecules in dashed boxes are suggested to be formed based on mass spectrometry (cf. Figure 1) and reported literature, see Ref. [9a].

scopy exhibit phenyl groups. Some examples are biphenyl or 2-phenylnaphtalene, which highlight the prevailing role of phenyl chemistry in the reactor. While allene has not been detected in the SPI TOF-MS (Figure 1a) due to its high IE,[26] its formation in **B** was predicted in theoretical work on reactions of chemically activated C_9H_9 isomers.[9a] The reverse reaction of **B** was computed to proceed with a barrier of just $+18$ kJ mol^{-1}.[9a]

Further pressure and temperature dependent dissociation reactions of **2** on the C_9H_9 potential energy surface (PES) were characterized by Vereecken and Peeters.[9b] Decomposition to indene (C_9H_8) + H was predicted as a dominant product along with additional exit channels, for example leading to phenylacetylene (C_8H_6) + CH_3. Both aromatics are identified in our study too, see Figure S6 and S7 in the Supporting Information. Furthermore, the reaction of allene with phenyl has also been observed to form indene in a VUV photoionization study.[27] The reaction was proposed to either proceed via **2** (reverse reaction of **B**) or a second resonantly stabilized C_9H_9 radical.[9a,27] The observation of indene is of considerable interest, as it is among the few PAH that have been identified unambiguously in interstellar space.[28]

In addition to the self-recombination reaction **A**, the reaction with phenyl radicals formed in **B** provides another efficient pathway for molecular growth at high temperature, known as the PAC mechanism.[29] Here, addition of a phenyl radical to an aromatic hydrocarbon is followed by successive dehydrogenation, cyclization and aromatization. The mechanism was already indicated by the pattern of the mass peaks in the REMPI TOF-MS (cf. Figure 1b) and is further substantiated by the identification of biphenyl (m/z 154), terphenyl (m/z 230), and triphenylene (m/z 228), see Figure 3 and Figure 4a. Preferentially, phenyl will add at the bay position of biphenyl.[3] The latter is itself a product of the self-reaction of phenyl.[30] Additionally, the disproportionation products of the phenyl self-reaction, benzene and *o*-benzyne,[31] might also contribute to the formation of biphenyl,[32] as the presence of benzene is suggested by the mass signal at m/z 78 in the SPI TOF-MS (cf. Figure 1a).

After phenyl addition, *o*-terphenyl could be formed by loss of an H atom.[3] However, the IR/UV spectrum of m/z 230 is clearly dominated by *p*-terphenyl, see Figure 3c-f. This is in agreement with a recent photoionization study by Zhao et al.,

who investigated the mechanism of the reaction of phenyl with biphenyl.[33] Yet, the formation of triphenylene (m/z 228, Figure 3a) will proceed via dehydrogenation and cyclization of *o*-terphenyl,[24,33] and thus likely accounts for its absence in the spectrum. A rapid conversion of the latter is further suggested thermochemically as *o*-terphenyl is slightly higher in energy than *p*- and *m*-terphenyl at 1000 K (cf. Figure 3). Although phenyl addition at the bay position is favored,[3] minor contributions to *p*-terphenyl by PAC are expected in addition to reaction **A**, since the initial addition reaction is also possible in the *para* position of the phenyl moiety of biphenyl.[24] Addition in the *meta* position is less likely due to a low electron density as known for aromatic radical substitution reactions,[24,34] explaining the absence of *m*-terphenyl in the IR/UV spectrum (see Figure 3c).

The identification of 2-phenylnaphthalene (cf. Figure 5c) further indicates efficient mass growth via PAC. Phenyl can add to the C1 or C2 carbon atom of naphthalene with computed $\Delta_R H^\circ = -137$ and -116 kJ mol^{-1} respectively, yielding 1- and 2-phenylnaphthalene after loss of H atom.[33] In our study, only the thermochemically more stable 2-substituted isomer is identified (Figure 5). Interestingly, naphthalene (m/z 128, Figure 5a) further reflects the dominant phenyl chemistry occurring in the reactor, as it can be formed by two phenyl units in a radical/π-bond addition reaction according to Equation (1):[30,32]

$$2\,C_6H_5 \rightarrow C_{10}H_8 + C_2H_2,\ \Delta_R H^\circ = -289\ \text{kJ mol}^{-1} \quad (1)$$

Furthermore, the reaction of propargyl (m/z 39) with a benzyl radical (m/z 91),[35] as well as the self-reaction of the cyclopentadienyl radical (m/z 65),[36] are known as primary routes for the formation of naphthalene. However, as neither m/z 39 nor 65 or 91 are observed in the TOF-MS (Figure 1), naphthalene formation via Equation (1) is most likely.

The generation of phenanthrene (m/z 178, Figure 4c) in combustion processes is expected to proceed via the acetylene-based HACA mechanism from biphenyl.[37] Furthermore, the addition of phenyl to phenylacetylene (see Figure S6 in the Supporting Information) via four-membered ring intermediates as a variation of the PAC mechanism[24,38] was reported as another efficient route.[39] Recently, the route was predicted to preferentially proceed via the formation of 2-ethynylbiphenyl by PAC, followed by H-assisted isomerization to phenanthrene.[40] Considering the significant amounts of phenyl in the reactor, this reaction is expected to occur. The less stable isomer anthracene has not been observed (see Figure 4c). This indicates that the PAH formation under the present conditions is mostly driven thermodynamically and the product with the lowest Gibbs energy is preferentially formed.

Recently, we investigated the high temperature chemistry of the 2-methylallyl[6] (2-MA) and 1- and 3-phenylpropargyl radicals[7] (1- and 3-PPR) in a microreactor. While 2-MA exhibits a methyl group instead of phenyl, PPR and **2** are composed of three C_3 units that play an important role in the formation of aromatic hydrocarbons.[41] Due to their close relation, similar reactions of the radicals are expected to be involved in molecular growth and thus are compared in the following.

Related to the work described here, unimolecular decomposition of 2-MA to methyl and allene (rather than phenyl and allene) has been observed as a key reaction to yield building blocks involved in the formation of larger aromatics.[6] Several reaction products were connected by addition of methyl groups, which suggests that methylation in the high temperature chemistry of 2-MA parallels the reactions observed in the present work.[6] While allene was experimentally identified by previous TPES work,[42] its formation due to **B** in the present study (see Scheme 2) was predicted by theoretical work[9a] and is indirectly concluded from the various reaction products with phenyl groups. Interestingly, a preferential addition of methyl and phenyl to naphthalene at the C2 carbon atom was found in both studies, indicating that formation of the 2-substituted naphthalene isomer is favored over its 1-substituted counterpart at high temperature.[6]

While dimerization of **2** is evident from the mass signal at m/z 234 in the SPI TOF-MS (Figure 1a), the recombination product of 2-MA was not observed in the TOF mass spectra,[6] but has been reported in previous work.[43] Yet, its formation was suggested by the generation of *p*-xylene via dehydrocyclization ($-H_2$) and aromatization ($-H_2$) of the latter.[6] A similar mechanism presumably leads to the formation of *p*-terphenyl starting from **3** in this work, see Scheme 2.

Interestingly, the self-reaction of 1- and 3-PPR[7] (C_9H_7, m/z 115) also leads to a predominant formation of *p*-terphenyl. Both radicals, **2** and PPR, efficiently form m/z 228, but different carriers of the mass signal have been identified in the two studies. **2** results in the formation of triphenylene (Figure 3a), while for both PPR isomers the m/z 228 product was assigned to 1-phenylethynyl naphthalene (1-PEN).[7,44] The selectivity of the self-reaction was traced back to a resonance stabilization of the radical positions.[7] In contrast to **2**, no decomposition of PPR to phenyl radicals has been observed. This might partly be traced to the greater stability of 1-PPR by 34.1 kJ mol^{-1} and of 3-PPR by 24.6 kJ mol^{-1} relative to **2**.[8a]

Furthermore, indene has been detected as a reaction product of PPR and is also observed here. Its formation from both radicals requires an initial isomerization. In PPR isomerization to indenyl is followed by addition of an H atom,[7] while loss of an H atom follows isomerization in **2**, as computed.[9b] The formation of indene in both cases demonstrates the high stability of the molecules.

Conclusion

The chemistry of the resonance-stabilized 2-phenylallyl radical (2-PA) in a high-temperature microreactor was investigated by IR/UV ion dip spectroscopy in a free jet using free electron laser radiation. 2-PA is considered as a potential intermediate in the formation of polycyclic aromatic hydrocarbons (PAH) at high temperature in combustion processes but might also be relevant in interstellar space. The radical was generated from a nitrite precursor and identified by its gas-phase IR spectrum in the fingerprint region. Several reaction products were also identified from their IR spectra with the aid of DFT computa-

tions, showing that uni- and bimolecular reactions of 2-PA contribute to molecular growth. In particular, three competing reactions of 2-PA were found to contribute to PAH formation. First, the radical self-reaction directly forms *p*-terphenyl. Such self-reactions often proceed barrierless and are thus promising pathways also for molecular growth in interstellar space. Second, unimolecular decomposition of 2-PA to allene and a phenyl radical produces the building blocks for PAH formation via the PAC mechanism (phenyl addition (dehydro-)cyclization) at high temperature. This pathway is evident from the identification of the reaction products biphenyl, terphenyl and triphenylene. Third, isomerization followed by H abstraction was computed to form indene.[9a] In all pathways, the thermodynamically favored isomer is formed. Furthermore, the high temperature chemistry was compared with the one of the 2-methylallyl and phenylpropargyl radicals, highlighting the similarities and differences in the high-temperature chemistry of the chemically related radicals.

Experimental Section

The experiments were carried out at the FELIX free electron laser laboratory[45] at the Radboud University, Nijmegen, The Netherlands. 2-phenylallyl (**2**) was generated by flash pyrolysis from 3-phenyl-but-3-en-1-yl nitrite **1**, see Scheme 1. The nitrite precursor, synthesized from but-3-yn-1-ol according to literature[46] (see Figure S9 in the Supporting Information), was heated to 115–125 °C in an in-vacuum molecular beam source, seeded in 2.5 bar of argon, and expanded into a differentially pumped vacuum apparatus[15] using a solenoid valve (Series 9, Parker General Valve) pulsed at 20 Hz. The latter was equipped with a resistively heated SiC tube (length: 40 mm, Ø: 1 mm, heated region: 10 mm) with a pyrolysis temperature of around 800 K to generate **2** and record its IR spectrum.[10] Subsequently, the temperature was increased to around 1000 K to promote further chemical reactions of **2** in the microreactor.[11–12] In the resulting free jet, molecules are adiabatically cooled to approximately room temperature. The jet was skimmed and crossed by perpendicular UV light and counterpropagating FEL-IR radiation in the interaction region of a reflectron time-of-flight mass spectrometer (R. M. Jordan Co.).[15] The UV light was provided by an unfocused Nd:YAG-laser pumped dye laser (Lioptec, operated at 20 Hz) followed by frequency doubling to perform [1 + 1]-REMPI at 270 nm (~1.5 mJ/pulse). To record IR/UV spectra[15] of the pyrolytically generated species, FELIX[45] was set around 200 ns prior to the UV laser and operated at 10 Hz to obtain alternating IR-OFF/IR-ON ion yields in the range of 560–1600 cm^{-1} in steps of 2 cm^{-1}. Note that FELIX (10 μs pulse) typically exhibits a bandwidth of around 1% of the central photon frequency with an output power of up to 150 mJ/pulse in the MIR region. The resulting mass-selected IR spectra were obtained by dividing the IR-OFF ion signal by the IR-ON ion signal, taking the decadic logarithm, correcting for IR laser power, averaging over several scans, and using digital Savitzky-Golay filtering. The experimental details for recording the TPE spectrum of **2** using synchrotron radiation are given in the Supporting Information.

The spectra were compared to harmonic vibrational DFT calculations at the B3LYP/6-311 + + G** level of theory[47] using the Gaussian16 computational chemistry software.[48] All computed spectra were scaled with an empirical factor of 0.985, which is in the range of values recommended by previous benchmark studies,[49] and convolved with a Gaussian-shaped function (FWHM = 24 cm^{-1}). Computations of standard heat of reactions of possible reactions occurring in the reactor as well as ionization energies were likewise performed at the DFT/B3LYP/6-311 + + G** level of theory. The relative Gibbs energies at 300 K and 1000 K of the structural isomers were computed at the same theoretical level employing the ORCA 5.0 software package.[50]

Acknowledgements

This work was supported by the German Science Foundation, DFG, through Graduiertenkolleg research training group GRK 2112. Furthermore, the research leading to these results has received funding from LASERLAB-EUROPE (grant agreement no. 654148, European Union's Horizon 2020 research and innovation programme). We gratefully thank the FELIX staff for their experimental support, and we acknowledge the Nederlandse Organisatie voor Wetenschappelijk Onderzoek (NWO) for the support of the FELIX Laboratory. Floriane Sturm acknowledges a fellowship by the Rosa Luxemburg Foundation. We further acknowledge the valuable help of Marius Gerlach, Floriane Sturm and Dr. Domenik Schleier in the measurement of the TPE spectrum of **2** at the Swiss Light Source. Open Access funding enabled and organized by Projekt DEAL.

Conflict of Interest

The authors declare no conflict of interest.

Data Availability Statement

The data that support the findings of this study are available from the corresponding author upon reasonable request.

Keywords: free electron laser · free jet · IR spectroscopy · PAH formation · radical reactions

[1] a) A. M. Mastral, M. S. Callen, *Environ. Sci. Technol.* **2000**, *34*, 3051–3057; b) H. Richter, V. Risoul, A. L. Lafleur, E. F. Plummer, J. B. Howard, W. A. Peters, *Environ. Health Perspect.* **2000**, *108*, 709–717.
[2] A. M. Ricks, G. E. Douberly, M. A. Duncan, *Astrophys. J.* **2009**, *702*, 301–306.
[3] R. I. Kaiser, N. Hansen, *J. Phys. Chem. A* **2021**, *125*, 3826–3840.
[4] K. O. Johansson, M. P. Head-Gordon, P. E. Schrader, K. R. Wilson, H. A. Michelsen, *Science* **2018**, *361*, 997–1000.
[5] T. W. Schmidt, *Int. Rev. Phys. Chem.* **2016**, *35*, 209–242.
[6] T. Preitschopf, F. Hirsch, A. K. Lemmens, A. M. Rijs, I. Fischer, *Phys. Chem. Chem. Phys.* **2022**, *24*, 7682–7690.
[7] K. H. Fischer, J. Herterich, I. Fischer, S. Jaeqx, A. M. Rijs, *J. Phys. Chem. A* **2012**, *116*, 8515–8522.
[8] a) T. P. Troy, N. Chalyavi, A. S. Menon, G. D. O'Connor, B. Fuckel, K. Nauta, L. Radom, T. W. Schmidt, *Chem. Sci.* **2011**, *2*, 1755–1765; b) J. A. Sebree, N. M. Kidwell, E. G. Buchanan, M. Z. Zgierski, T. S. Zwier, *Chem. Sci.* **2011**, *2*, 1746–1754.
[9] a) L. Vereecken, J. Peeters, *Phys. Chem. Chem. Phys.* **2003**, *5*, 2807–2817; b) L. Vereecken, J. Peeters, H. F. Bettinger, R. I. Kaiser, P. V. Schleyer, H. F. Schaefer, *J. Am. Chem. Soc.* **2002**, *124*, 2781–2789.
[10] D. W. Kohn, H. Clauberg, P. Chen, *Rev. Sci. Instrum.* **1992**, *63*, 4003–4005.
[11] Q. Guan, K. N. Urness, T. K. Ormond, D. E. David, G. B. Ellison, J. W. Daily, *Int. Rev. Phys. Chem.* **2014**, *33*, 447–487.

[12] a) A. Vasiliou, M. R. Nimlos, J. W. Daily, G. B. Ellison, *J. Phys. Chem. A* **2009**, *113*, 8540–8547; b) A. M. Scheer, C. Mukarakate, D. J. Robichaud, G. B. Ellison, M. R. Nimlos, *J. Phys. Chem. A* **2010**, *114*, 9043–9056.
[13] a) F. T. Zhang, R. I. Kaiser, A. Golan, M. Ahmed, N. Hansen, *J. Phys. Chem. A* **2012**, *116*, 3541–3546; b) D. S. N. Parker, R. I. Kaiser, B. Bandyopadhyay, O. Kostko, T. P. Troy, M. Ahmed, *Angew. Chem. Int. Ed.* **2015**, *54*, 5421–5424; *Angew. Chem.* **2015**, *127*, 5511–5514; c) D. S. N. Parker, R. I. Kaiser, T. P. Troy, M. Ahmed, *Angew. Chem. Int. Ed.* **2014**, *53*, 7740–7744; *Angew. Chem.* **2014**, *126*, 7874–7878.
[14] a) P. Hemberger, A. Bodi, *Chimia* **2018**, *72*, 227–232; b) I. Fischer, S. T. Pratt, *Phys. Chem. Chem. Phys.* **2022**, *24*, 1944–1949.
[15] A. M. Rijs, J. Oomens, *Top. Curr. Chem.* **2014**, *364*, 1–42.
[16] F. Hirsch, P. Constantinidis, I. Fischer, S. Bakels, A. M. Rijs, *Chem. Eur. J.* **2018**, *24*, 7647–7652.
[17] F. Hirsch, E. Reusch, P. Constantinidis, I. Fischer, S. Bakels, A. M. Rijs, P. Hemberger, *J. Phys. Chem. A* **2018**, *122*, 9563–9571.
[18] A. K. Lemmens, D. B. Rap, J. M. M. Thunnissen, B. Willemsen, A. M. Rijs, *Nat. Commun.* **2020**, *11*.
[19] a) T. A. Cool, J. Wang, K. Nakajima, C. A. Taatjes, A. McIlroy, *Int. J. Mass Spectrom.* **2005**, *247*, 18–27; b) B. Yang, J. Wang, T. A. Cool, N. Hansen, S. Skeen, D. L. Osborn, *Int. J. Mass Spectrom.* **2012**, *309*, 118–128.
[20] A. D. Baker, C. Baker, C. R. Brundle, D. W. Turner, *Intern. J. Mass. Spectrom. Ion Phys.* **1968**, *1*, 285–301.
[21] a) O. P. Haefliger, R. Zenobi, *Anal. Chem.* **1998**, *70*, 2660–2665; b) J. E. Rink, U. Boesl, *Eur. J. Mass Spectrom.* **2003**, *9*, 23–32.
[22] a) A. M. Rijs, M. Kabeláč, A. Abo-Riziq, P. Hobza, M. S. de Vries, *ChemPhysChem* **2011**, *12*, 1816–1821; b) A. M. Rijs, G. Ohanessian, J. Oomens, G. Meijer, G. von Helden, I. Compagnon, *Angew. Chem. Int. Ed.* **2010**, *49*, 2332–2335; *Angew. Chem.* **2010**, *122*, 2382–2385; c) A. M. Rijs, N. Sandig, M. N. Blom, J. Oomens, J. S. Hannam, D. A. Leigh, F. Zerbetto, W. J. Buma, *Angew. Chem. Int. Ed.* **2010**, *49*, 3896–3900; *Angew. Chem.* **2010**, *122*, 3988–3992.
[23] M. Schmitt, F. Spiering, V. Zhaunerchyk, R. T. Jongma, S. Jaeqx, A. M. Rijs, W. J. van der Zande, *Phys. Chem. Chem. Phys.* **2016**, *18*, 32116–32124.
[24] B. Shukla, M. Koshi, *Phys. Chem. Chem. Phys.* **2010**, *12*, 2427–2437.
[25] a) D. A. Hrovat, J. G. Chen, K. N. Houk, W. T. Borden, *J. Am. Chem. Soc.* **2000**, *122*, 7456–7460; b) S. Sakai, *J. Mol. Struct.* **2002**, *583*, 181–188.
[26] R. Stockbauer, K. E. Mcculloh, A. C. Parr, *Int. J. Mass Spectrom. Ion Phys.* **1979**, *31*, 187–189.
[27] F. T. Zhang, R. I. Kaiser, V. V. Kislov, A. M. Mebel, A. Golan, M. Ahmed, *J. Phys. Chem. Lett.* **2011**, *2*, 1731–1735.
[28] A. M. Burkhardt, K. L. K. Lee, P. B. Changala, C. N. Shingledecker, I. R. Cooke, R. A. Loomis, H. J. Wei, S. B. Charnley, E. Herbst, M. C. McCarthy, B. A. McGuire, *Ap. J. Lett.* **2021**, *913*.
[29] M. Shukla, A. Susa, A. Miyoshi, M. Koshi, *J. Phys. Chem. A* **2008**, *112*, 2362–2369.
[30] P. Constantinidis, H. C. Schmitt, I. Fischer, B. Yan, A. M. Rijs, *Phys. Chem. Chem. Phys.* **2015**, *17*, 29064–29071.
[31] R. S. Tranter, S. J. Klippenstein, L. B. Harding, B. R. Giri, X. L. Yang, J. H. Kiefer, *J. Phys. Chem. A* **2010**, *114*, 8240–8261.
[32] A. Comandini, K. Brezinsky, *J. Phys. Chem. A* **2011**, *115*, 5547–5559.
[33] L. Zhao, M. B. Prendergast, R. I. Kaiser, B. Xu, U. Ablikim, M. Ahmed, B. J. Sun, Y. L. Chen, A. H. H. Chang, R. K. Mohamed, F. R. Fischer, *Angew. Chem. Int. Ed.* **2019**, *58*, 17442–17450; *Angew. Chem.* **2019**, *131*, 17603–17611.
[34] A. C. Brown, J. Gibson, *J. Chem. Soc. Trans.* **1892**, *61*, 367–369.
[35] W. Yuan, Y. Li, P. Dagaut, J. Yang, F. Qi, *Combust. Flame* **2015**, *162*, 3–21.
[36] G. Blanquart, P. Pepiot-Desjardins, H. Pitsch, *Combust. Flame* **2009**, *156*, 588–607.
[37] a) T. Yang, R. I. Kaiser, T. P. Troy, B. Xu, O. Kostko, M. Ahmed, A. M. Mebel, M. V. Zagidullin, V. N. Azyazov, *Angew. Chem. Int. Ed.* **2017**, *56*, 4515–4519; *Angew. Chem.* **2017**, *129*, 4586–4590; b) L. Zhao, R. I. Kaiser, B. Xu, U. Ablikim, M. Ahmed, D. Joshi, G. Veber, F. R. Fischer, A. M. Mebel, *Nat. Astron.* **2018**, *2*, 413–419.
[38] J. Aguilera-Iparraguirre, W. Klopper, *J. Chem. Theory Comput.* **2007**, *3*, 139–145.
[39] Z. P. Li, P. Liu, P. Zhang, H. He, S. H. Chung, W. L. Roberts, *J. Phys. Chem. A* **2019**, *123*, 10323–10332.
[40] L. B. Tuli, A. M. Mebel, *Int. J. Chem. Kinet.* **2020**, *52*, 875–883.
[41] J. A. Miller, S. J. Klippenstein, *J. Phys. Chem. A* **2003**, *107*, 7783–7799.
[42] M. Lang in *Valence Shell Photoionization of Soot Precursors with Synchrotron Radiation*, *Vol.* University of Wuerzburg, Wuerzburg, **2015**, p. 173.
[43] R. S. Tranter, A. W. Jasper, J. B. Randazzo, J. P. A. Lockhart, J. P. Porterfield, *Proc. Combust. Inst.* **2017**, *36*, 211–218.
[44] M. L. Hebestreit, C. Henrichs, J. Schafer, J. Martini, J. Auerswald, I. Fischer, A. Krueger, M. Schmitt, *J. Mol. Struct.* **2022**, *1250*.
[45] D. Oepts, A. F. G. van der Meer, P. W. Van Amersfoort, *Infrared Phys. Technol.* **1995**, *36*, 297–308.
[46] a) C. Shu, R. S. Mega, B. J. Andreassen, A. Noble, V. K. Aggarwal, *Angew. Chem. Int. Ed.* **2018**, *57*, 15430–15434; *Angew. Chem.* **2018**, *130*, 15656–15660; b) M. Gasser, J. A. Frey, J. M. Hostettler, A. Bach, *Chem. Commun.* **2011**, *47*, 301–303.
[47] R. Krishnan, J. S. Binkley, R. Seeger, J. A. Pople, *J. Chem. Phys.* **1980**, *72*, 650–654.
[48] Gaussian 16, Revision C.01, M. J. Frisch, G. W. Trucks, H. B. Schlegel, G. E. Scuseria, M. A. Robb, J. R. Cheeseman, G. Scalmani, V. Barone, G. A. Petersson, H. Nakatsuji, X. Li, M. Caricato, A. Marenich, J. Bloino, B. G. Janesko, R. Gomperts, B. Mennucci, H. P. Hratchian, J. V. Ortiz, A. F. Izmaylov, J. L. Sonnenberg, D. Williams-Young, F. Ding, F. Lipparini, F. Egidi, J. Goings, B. Peng, A. Petrone, T. Henderson, D. Ranasinghe, V. G. Zakrzewski, J. Gao, N. Rega, G. Zheng, W. Liang, M. Hada, M. Ehara, K. Toyota, R. Fukuda, J. Hasegawa, M. Ishida, T. Nakajima, Y. Honda, O. Kitao, H. Nakai, T. Vreven, K. Throssell, J. A. Montgomery, J. E. Peralta, F. Ogliaro, M. Bearpark, J. J. Heyd, E. Brothers, K. N. Kudin, V. N. Staroverov, T. Keith, R. Kobayashi, J. Normand, K. Raghavachari, A. Rendell, J. C. Burant, S. S. Iyengar, J. Tomasi, M. Cossi, J. M. Millam, M. Klene, C. Adamo, R. Cammi, J. W. Ochterski, R. L. Martin, K. Morokuma, O. Farkas, J. B. Foresman, D. J. Fox, *Gaussian, Inc., Wallingford CT* **2016**.
[49] M. L. Laury, M. J. Carlson, A. K. Wilson, *J. Comput. Chem.* **2012**, *33*, 2380–2387.
[50] F. Neese, *WIREs Comput. Mol. Sci.* **2022**, *12*, e1606.

Manuscript received: September 20, 2022
Accepted manuscript online: December 8, 2022
Version of record online: February 1, 2023